DISCOVERY OF A REMARKABLE POINT-SYMMETRIC PROTOPLANETARY NEBULA: HST IMAGING OF IRAS04296+3429

Raghvendra Sahai[1]

Received _____; accepted _____

[1]Jet Propulsion Laboratory, MS 183-900, California Institute of Technology, Pasadena, CA 91109

ABSTRACT

We present images of the protoplanetary nebula (PPN) IRAS04296+3429 taken with the Hubble Space Telescope Wide-Field Planetary Camera 2 in two wide-band filters centered at 0.54 and 0.81μm. We find that this object, which belongs to a class of carbon-rich PPNs with a peculiar 21μm dust emission feature, has a striking point-symmetric morphology, with a pair of long well-collimated lobes oriented at about 70° to an equatorial elliptical "disk" like structure. Although dense disk-like regions have been inferred from the presence of dark lanes separating the bipolar lobes of post-AGB objects, I04296 is the first to show a bounded disk directly in scattered light. The lobes and the disk appear embedded in a roughly round, faint halo with a radius at least as large as 2.″8. The bipolar lobes probably result from the interaction of a collimated high-velocity bipolar outflow with the spherical progenitor AGB circumstellar envelope, seen as the halo. The internal structure of the lobes suggests that the bipolar outflow changes its direction with time. A simple single-scattering model of a spherical inverse-square density envelope with a dust mass-loss rate of $4\times10^{-8}M_{\odot}$ yr^{-1}provides a good fit to the scattered light in the halo at both wavelengths. The collimated lobes and point-symmetric structure in I04296 provide strong support for jet-driven formation of aspherical planetary nebulae.

Subject headings: planetary nebulae, stars: AGB and post–AGB, stars: mass–loss, circumstellar matter

1. Introduction

Most planetary nebulae (PN) show significant departures from spherical symmetry [e.g. Aaquist & Kwok 1991, Schwarz, Corradi, & Melnick et al. 1992, Sahai & Trauger 1998 (hereafter ST98)], whereas the circumstellar envelopes (CSEs) of their progenitor AGB stars appear spherically symmetric (e.g. Bowers, Johnston, & Spencer 1983, Neri et al. 1998). Why and how this happens is not well understood. Although several theoretical mechanisms have been proposed (e.g.Balick 1987, Chevalier & Luo 1994, Morris 1987), the discoveries of fast low ionisation emission regions (FLIERs: Balick et al. 1998), and multipolar/point-symmetric structures (e.g. ST98), strongly suggest that additional/new shaping mechanisms are required. ST98 have proposed that collimated fast outflows with changing directionality, operating during the very late-AGB or the early post-AGB (hereafter protoplanetary phase), are the primary agents in the formation of aspherical PNs. Using the Wide Field and Planetary Camera 2 (WFPC2) onboard HST, it has now become possible to image protoplanetary nebulae (PPN) in scattered light with unprecedented angular resolution and dynamic range (Sahai et al. 1998, Sahai et al. 1999a,b,c; Kwok, Su, & Hrivnak 1998, Su et al 1998). Such observations provide stringent constraints on the nature and history of mass-loss during AGB and early post-AGB evolution, crucial for testing our ideas for the formation and shaping of PN. For example, our HST images of the PPN Hen401 reveal a pair of very long, highly collimated lobes, supporting our viewpoint that jet-like outflows shape planetary nebulae (Sahai et al. 1999c, hereafter SBZ99).

IRAS04296+3429 (hereafter I04296) is a well-studied member of a class of PPN with a peculiar 21μm emission feature in their IRAS low-resolution spectra (Kwok 1993, Kwok, Volk, & Hrivnak 1989). Spectral features due to C_2, C_3 and *s*-process elements show that I04296 is an evolved carbon-rich object (Hrivnak 1995), and mm-wave molecular line emission (Omont et al. 1993, Woodworth et al. 1990) reveals the presence of a dense AGB

CSE with an expansion velocity, V_{exp}=(12–15.6) km s^{-1}. Although spectropolarimetry indicates an aspherical dust distribution in I04296 (Trammell, Dinerstein & Goodrich 1994), its structure has remained unknown. Mid-infrared (9.7 and 11.8μm) images (Meixner et al 1997 show an unresolved object. The distance to I04296 is not known; we adopt D=4 kpc as suggested by Meixner et al 1997 based on assuming a typical PPN luminosity of $5.3\times10^3 L_\odot$. In this Letter, we present HST images of I04296 - the remarkable morphology we find has important implications for theories of PN shaping and formation.

2. Observations and Data Reduction

A total of 6 exposures of I04296 (2×1.6 s, 2×20 s, 2×200 s) using two broad-band filters [F555W ($<\lambda>$=0.54μm, $\delta\lambda$=0.12μm) and F814W ($<\lambda>$=0.79μm, $\delta\lambda$=0.15μm)], taken as part of an HST SNAPshot imaging program (6364: Bobrowsky) and processed via the standard calibration pipeline, were retrieved from HST archives. The nebula lies within the Planetary Camera (800^2 pixels; plate scale=0.″0456/pixel) of WFPC2. Each image of an equal exposure pair was shifted with respect to the other during the observations. After applying a geometric distortion correction, the images were registered to sub-pixel accuracy (using cross-correlation techniques), followed by cosmic ray removal and correction of saturated pixels in the long exposure images.

3. Results

The nebula, seen in scattered light, shows a pair of long well-collimated lobes oriented along PA≈98°, and an equatorial elliptical "disk" like structure with a major axis (1.″6 long) oriented at PA=28° (Fig. 1 a,b). Although the existence of dense dusty disk-like structures has generally been inferred from the dark lanes separating the bipolar lobes of post-AGB

objects in optical/near-infrared images, I04296 is the first to show a *bounded* disk directly in scattered light. Each bipolar lobe (radial extent of about 1.″9) contains an inner lobe (radial extent about 0.″7): the latter can be seen more clearly in panels *c* & *d* of Fig. 1, which emphasize sharp structures. The bipolar lobes are not exactly colinear: there is a small difference of about 5° between their axes. The inner lobes are aligned along an axis which is slightly different than that of the outer lobes. The lobes and the disk appear embedded in a roughly round, faint halo, which extends to a sensitivity-limited (3σ) radius of about 2.″8 in the F814W image. The central star can be seen as the bright point source at the nebular center. We determine m_V=14.1 (consistent with m_V=14.2 determined by Hrivnak 1995), and m_I=11.6, for the nebula as a whole (including the central star). If we assume that the elliptical disk is intrinsically circular and geometrically thin, its minor-to-major axis ratio implies that the disk-plane is inclined to our line-of-sight (*los*) by 24°. In view of its visual appearance, we hereby name I04296 as the "Seagull Nebula".

The central star, which is resolved from surrounding nebulosity, shows a F555W/F814W count rate ratio of 0.16±0.01, significantly smaller than that expected (1.2) from its G0 spectral type (Hrivnak 1995), implying that it is significantly reddened due to nebular extinction along the *los* to the star. We estimate this extinction in two ways: first, comparing the observed F555W/F814W count rate ratio with that expected with no extinction, and using the standard interstellar extinction curve (Whittet 1992), we find an extinction optical depth at 0.56μm, τ_{555}=4.5. Second, we compare the observed stellar fluxes with estimates based on its bolometric flux (1.1×10^{-8} erg s^{-1} cm^{-2}) and effective temperature (5500K). We determine m_V=16.3 & m_I=13.4 for the central star, implying 0.56 & 0.81μm fluxes of 1 & 9.6 mJy, respectively. Since the corresponding unattenuated fluxes are 1.35 and 1.97 Jy, we derive extinction optical depths τ_{555}=7.2 & τ_{814}=5.3. Thus there is a large discrepancy between the extinction estimated by the above two methods which cannot be accounted for by uncertainties in the observed or intrinsic stellar flux

values. The τ_{555}/τ_{814} ratio from method 2 (1.36) is smaller than that derived from method 1 (1.6); hence the extinction curve between 0.56 and 0.81μm for dust grains along the *los* to the central star is flatter than the interstellar one. We conclude that these grains, most likely residing in the equatorial "disk" region, have a radius significantly larger than the nominal value ($\sim$ 0.1μm) for interstellar grains. Two other well-studied PPNs, CRL2688 and the Red Rectangle (Sahai et al. 1998, Jura, Turner, & Balm 1997), show evidence for large grains in their dense equatorial regions.

4. Modelling of Scattered Light

In Figure 2, we show the F555W/F814W ratio image. The bipolar lobes, with large ($\sim$0.19-0.24) values of the 0.55μm to 0.81μm flux ratio ($R_{555/814}$) stand out clearly from the rest of the nebula (equatorial disk and halo), which is characterised by $R_{555/814}$ $\sim$0.12-0.18. $R_{555/814}$ is smallest towards the central star, implying that it is significantly redder than all of the surrounding nebulosity, specially the bipolar lobes, which show the largest $R_{555/814}$ ratio. We conclude that the starlight reaching us directly undergoes the largest extinction (presumably due to the disk), and that reaching the bipolar lobes undergoes the least.

In Figure 3, we show four representative radial cuts from the F555W/F814W ratio image. The variation of the ratio in the "disk cuts", taken along the disk major axis is distinctly different from that in the "halo cuts". The latter have been taken along directions about 116° away from the "disk cuts", in order to minimise the disk contribution and avoid the bipolar lobes and diffraction spikes in the image. The ratio in the "halo cuts" shows a roughly steady rise, whereas in the "disk cuts", it varies around a roughly fixed value up to a radius of about 0.″8, and then shows a distinct rise. The break near 0.″8 is probably related to the different dust properties and optical depths in the dusty equatorial disk which has a radius of about 0.″8. The halo intensity for radius $r \gtrsim$ 0.″25 is found to vary roughly as

$I_0(r/1'')^{-\beta}$, with $I_0 = 95$ μJy arsec^{-2} & $\beta \sim (2.8 - 3.0)$ at 0.56μm and $I_0 = 650$ μJy arsec^{-2} & $\beta \sim (3.0 - 3.2)$ at 0.81μm. Since optically-thin scattering in a spherical CSE with a $r^{-\alpha}$ density law produces an $r^{-(\alpha+1)}$ intensity variation, we conclude that the I04296 CSE is characterised by $\alpha \sim 2$ (consistent with steady mass-loss at a constant expansion velocity) and relatively small scattering optical depths for $r \gtrsim 0''.25$.

We present a simple single-scattering model of such a CSE that fits the salient characteristics of the F555W/F814W ratio and intensities in the halo. The inputs to our model are the (i) dust mass-loss rate, (ii) the radial extinction at 0.56μm, $\tau_{ext,1''}$, from the star to a nominal radius of 1", and (ii) the dust grain properties. For the latter, we assumed (i) isotropic scattering with a cross-section of 2.1×10^4 cm^2 g^{-1} (i.e. *per unit dust mass*) and an albedo of 0.57 at 0.6μm (e.g. Martin & Rogers 1987), and (ii) a λ^{-4} (λ^{-1}) variation of the scattering (absorption) cross-section over the wavelength range covered by the two filters. The radial rise in the halo F555W/F814W ratio results from the slower radial fall-off of the F555W intensity, compared to F814W, due to the higher opacity at shorter wavelengths. We find that the "halo cuts" and the observed intensities can be reasonably fit with $\tau_{ext,1''}$=4.4 and a CSE dust mass-loss rate of $4\times10^{-8}(15.6 \text{ km s}^{-1}/V_{exp})M_\odot$ yr^{-1}. Assuming a gas-to-dust ratio of 200 for AGB CSEs, the total AGB mass-loss rate in I04296 is about $8\times10^{-6}M_\odot$ yr^{-1}, consistent with values derived from CO data. We have chosen not to independently constrain the dust mass and mass-loss rate from the IRAS far-infrared fluxes, because the strong 21μm feature invalidates the use of our simple *power-law* dust emissivity model (e.g. Sahai et al. 1991).

5. The Structure of I04296

The morphology of I04296 seen in the HST images dramatically reveals the transition from spherical AGB mass-loss to highly-collimated mass-outflow. The long, narrow bipolar

lobes in I04296 are probably produced by the interaction of a collimated high-velocity bipolar outflow with the spherical progenitor AGB CSE, which appears as the round halo in the HST images. The internal structure of the lobes is reminiscent of the multiple-outflow lobes of high-velocity gas seen in the young PN M1-16 (Schwarz 1992). Such lobes can be produced by intrinsically-collimated (i.e. close to the star) jet-like outflows which change their direction with time, as proposed by ST98. Although the mechanism(s) for producing the jets is unclear, several hypotheses exist which directly or indirectly require the presence of close stellar/sub-stellar companions (e.g. see ST98). Indirect evidence for fast-moving material in I04296 comes from the presence of an emission feature at λ4071, possibly due to the [SII] blend of λ4069 and λ4076 (Hrivnak 1995): such emission is expected to arise in shocked gas resulting from the fast outflow interaction with the AGB CSE. The bipolar lobes in I04296 have "closed ends", indicating that the high-velocity outflow has not "broken out" as yet from the confining AGB CSE. In contrast, the bipolar lobes of the more evolved PPN, Hen401, have open, tattered ends and a well-developed shell structure (SBZ99), indicating that the bipolar outflow in I04296 is either dynamically younger and/or less powerful than that in Hen401. The specific geometric shape of the lobes, in particular the narrowing of their ends, suggests "weak" deceleration of the hypothesised jet (de Young, *priv. comm.*) and "strong" cooling of the resulting shocked material (Masson & Chernin 1993). However, numerical hydrodynamic simulations are needed to test these ideas.

It is difficult to explain the structure of I04296 using the generalised interacting stellar winds ("GISW") model for the formation of aspherical PNs (Balick 1987). In this model, various *axisymmetric* nebular shapes are obtained by the interaction of a very fast isotropic central-star wind with the progenitor AGB CSE (Kwok 1982), when the latter is denser near the equator than the poles (Balick 1987). In contrast, I04296 shows a *point-symmetric* morphology: the bipolar lobes are *not* orthogonal to the equatorial disk. Second, none of the existing GISW simulations of PNs to-date (Mellema 1995 and references therein) have

produced the kind of long, narrow, outflow lobes we find in I04296 (and Hen401, see SBZ99). Although narrow jets can be produced hydrodynamically in GISW models using compact toroidal density distributions (Mellema & Frank 1997) or in magnetised wind-blown bubble models (Garcia-Segura 1997), the misalignment of the disk and lobes argues against, or, for significant modifications to, such models. Thus, HST imaging of I04296 and other PPNs such as Hen401 and IRAS16342 (Sahai et al. 1999b) should provide a strong impetus for extending theoretical studies of mechanisms for producing aspherical planetary nebulae, specially jet-driven (e.g. Steffen & Lopez 1998) and magneto-hydrodynamic models.

The origin of the disk in I04296 remains a puzzle. Its large size and sharp outer edge potentially sets strong constraints on mechanisms for the production of dense equatorial structures around AGB stars (e.g. Morris 1987, Livio 1993). The large radius of the disk ($\sim few \times 10^{16}$ cm) makes wind-accretion by a close compact companion an unlikely explanation. We think that the disk signifies a qualitative and temporally-sharp change in the mass-ejection proces, e.g. due to an evolutionary event such as a binary merger leading to common-envelope ejection (e.g. Soker & Livio 1994). Such an event could plausibly lead to the expansion of material along a preferred plane at high speeds; the resulting shock in the ambient dense AGB CSE would then define the sharp edge of the disk.

The author thanks Valentin Bujarrabal, Dave de Young and Mark Morris for comments on the paper, and NASA for financial support from a Long Term Space Astrophysics grant (no. 399-30-61-00-00).

REFERENCES

Aaquist & Kwok 1991, ApJ, 378, 599

Balick, B. 1987, AJ, 94, 671

Balick, B., Alexander, J., Hajian, A.R., Terzian, Y., Perinotto, M., & Patriarchi, P. 1998, AJ, 116, 360

Bowers, P.F., Johnston, K.J., & Spencer, J.H. 1983, ApJ, 274, 733

Chevalier, R.A. & Luo, D. 1994, ApJ, 421, 225

Garcia-Segura, G. 1997, ApJ, 489, L189

Hrivnak, B.J. 1995, ApJ, 438, 341

Jura, M., Balm, S.P., & Kahane, C. 1995, ApJ, 453, 721

Jura, M., Turner, J. & Balm, S.P. 1997, ApJ, 474, 741

Kwok, S. 1982, ApJ, 258, 280

Kwok, S. 1993, ARA&A, 31, 63

Kwok, S., Su, K.Y.L., & Hrivnak, B. 1998, ApJ, 501, L117

Kwok, S.,Volk, K.M., & Hrivnak, B.J. 1989, ApJ, 345, L51

Livio, M. 1993, in IAU Symp. 155, Planetary Nebulae, ed. R. Weinberger $ A. Acker (Dordrecht: Kluwer), 279

Martin, P. G. & Rogers, C. 1987, ApJ, 322, 374

Masson, C.R. & Chernin, L.M. 1993, ApJ, 414, 230

Mastrodemos, N. & Morris, M. 1998, 497, 303

Mellema, G. 1995, MNRAS, 277, 173

Mellema, G. & Frank, A. 1997, MNRAS, 292, 795

Meixner, M. Skinner, C.J., Graham, J.R., Keto, E., Jernigan, J.G., & Arens, J.F. 1997, ApJ, 482, 897

Morris, M. 1987, PASP, 99, 1115

Neri, R., Kahane, C., Lucas, R., Bujarrabal, V., & Loup, C. 1998, A&ASS, 130, 1

Omont, A., Loup, C., Forveille, T., te Lintel Hekkert, P., Habing, H., & Sivagnanam, P. 1993, A&A, 267, 515

Sahai, R., Wootten, A., Schwarz, H.E., & Clegg, R.E.S. 1991, A&A, 251, 560

Sahai, R., et al., 1998, ApJ, 493, 301

Sahai, R. & Trauger, J.T. 1998, AJ, 116, 1357

Sahai, R., Zijlstra, A., Bujarrabal, V., te Lintel Hekkert, P. 1999a, AJ, 117, 1408

Sahai, R., te Lintel Hekkert, P., Morris, M., Zijlstra, A., Likkel, L. 1999b, ApJ, 514, L115

Sahai, R., Bujarrabal, V., & Zijlstra, A., 1999c, ApJ, 518, L115

Schwarz, H.E., 1992, A&A, 264, L1

Schwarz, H.E., Corradi, R.J.M. & Melnick, J. 1992, A&AS, 96, 23

Soker, N. & Livio, M. 1994, ApJ, 421, 219

Steffen, W. & Lopez, J.A. 1998, ApJ, 508, 696

Su, K.Y.L., Volk, K., Kwok, S., Hrivnak, B.J. 1998, ApJ, 508, 744

Trammell, S.R., Dinerstein, H.L., & Goodrich, R.W. 1994, AJ, 108, 984

Whittet, D.C.B. 1992, *Dust in the Galactic Environment*, Institute of Physics Publishing, (Bristol, Philadelphia & New York), pp. 67

Woodworth, A.W., Kwok, S., Chan, S.J. 1990, A&A, 228, 503

This manuscript was prepared with the AAS LaTeX macros v4.0.

Fig. 1.— (a,b) Wide-band (F555W & F814W) images of the protoplanetary nebula IRAS04296+3429 taken with the Planetary Camera (resolution 0.″0456/pixel) of WFPC2/HST. A reverse grey-scale and logarithmic stretch have been used, with the maximum and minumum surface brightnesses on the scale bar for F555W (F814W) being 0.064 (0.54) Jy arcsec^{-2} & 0.023 (0.054) mJy arcsec^{-2}. (c,d) False-color images generated by processing the images in (a,b) in order to emphasize sharp structures. Each processed image, $Im_P = Im_O/(Im_O+0.04Im_S)$, where Im_O is the original image, and Im_S is obtained by smoothing Im_O. Diffraction artifacts due to telescope optics are seen prominently in the F814W image (at ±45° to the horizontal axis), but are much fainter than the nebular lobes in the F555W image, and do not affect our conclusions about their structure (§3 of text).

Fig. 2.— F555W/F814W intensity ratio image of IRAS04296+3429. The ratio scale is shown alongside.

Fig. 3.— Representative radial cuts from the F555W/F814W ratio image. The red curves show the "disk cuts" taken along the major axis of the elliptical disk (in 10° wide slices). The green curves show the "halo cuts", taken along directions about 116° away from the "disk cuts" (in 20° wide slices). The intensity computed from a simple single-scattering model of a spherical circumstellar envelope with a r^{-2} density law fits the "halo cuts".

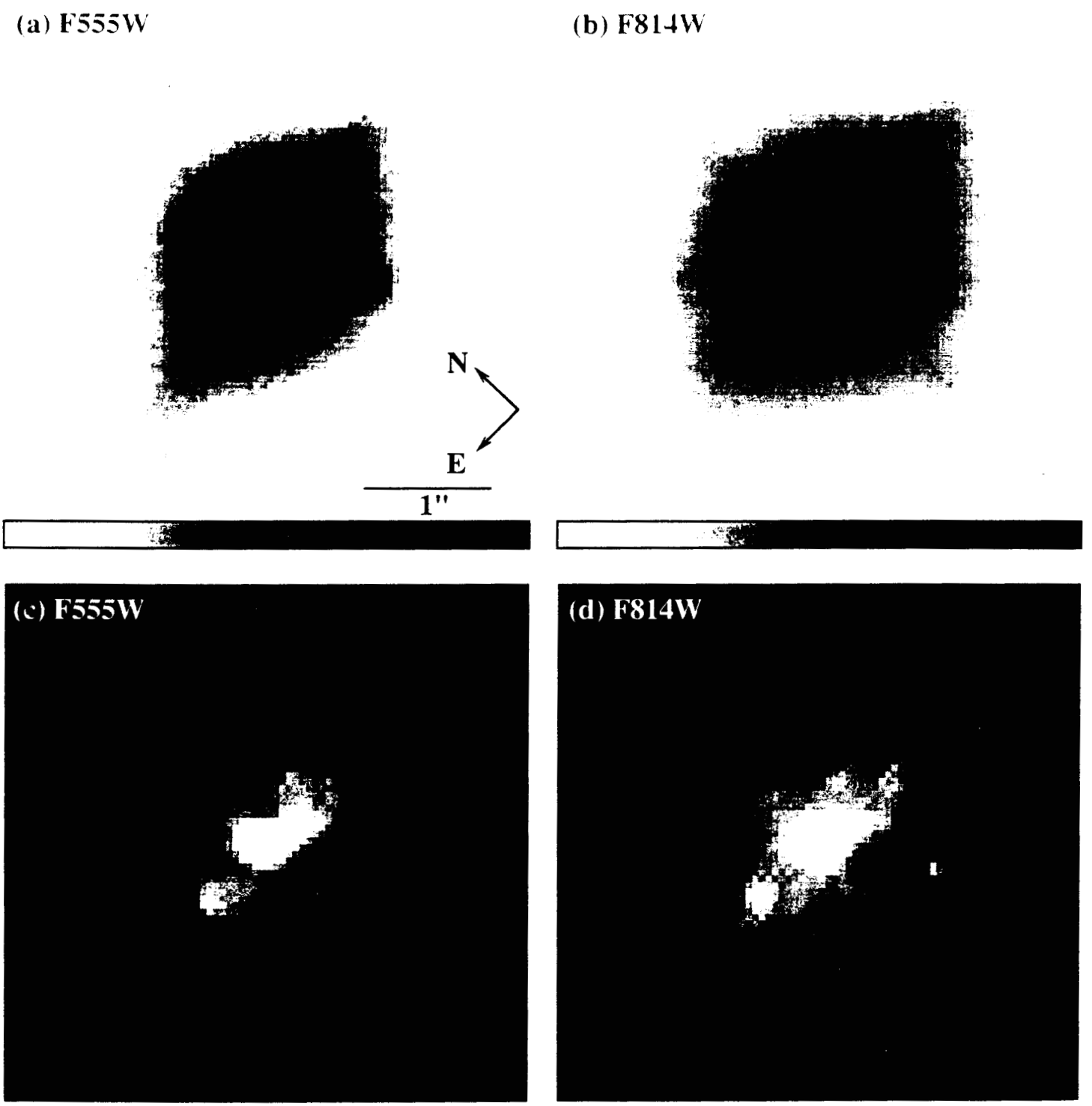
(a) F555W
(b) F814W
N
E
1"
(c) F555W
(d) F814W

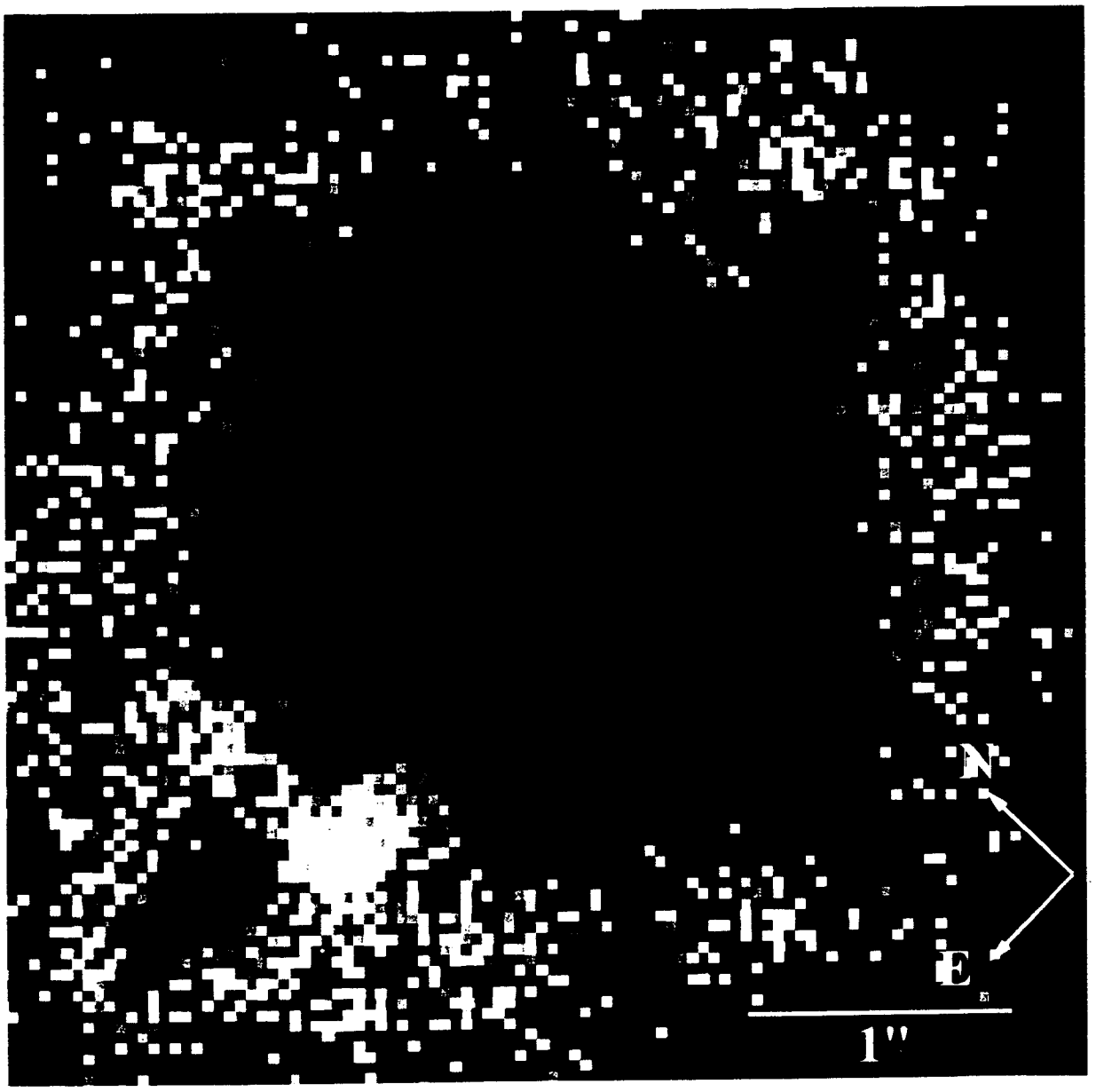
N
E
1"

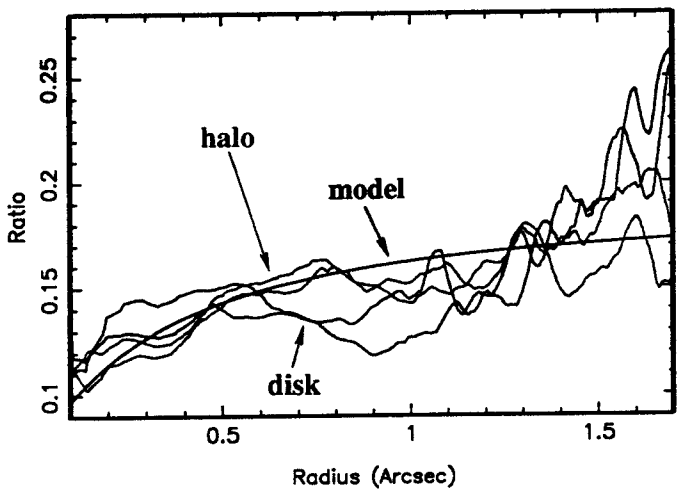
halo
model
disk
Ratio
0.1
0.15
0.2
0.25
0.5
1
1.5
Radius (Arcsec)